Acta Crystallographica Section F
Structural Biology and Crystallization Communications
ISSN 1744-3091

Structure of *Plasmodium falciparum* ADP-ribosylation factor 1

William J. Cook,[a] Craig D. Smith,[a] Olga Senkovich,[a] Anthony A. Holder[b] and Debasish Chattopadhyay[a]*

[a]University of Alabama at Birmingham, Birmingham, AL 35294, USA, and [b]Division of Parasitology, MRC National Institute for Medical Research, Mill Hill, London NW7 1AA, England

Correspondence e-mail: debasish@uab.edu

Received 30 June 2010
Accepted 15 September 2010

PDB Reference: ARF1 GTPase, 3lrp.

This article is dedicated to the memory of Dr Craig D. Smith.

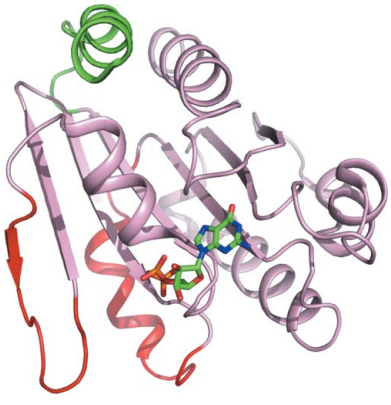

Vesicular trafficking may play a crucial role in the pathogenesis and survival of the malaria parasite. ADP-ribosylation factors (ARFs) are among the major components of vesicular trafficking pathways in eukaryotes. The crystal structure of ARF1 GTPase from *Plasmodium falciparum* has been determined in the GDP-bound conformation at 2.5 Å resolution and is compared with the structures of mammalian ARF1s.

1. Introduction

The protozoan parasite *Plasmodium falciparum* was responsible for over 90% of the approximately one million deaths from malaria in 2008 (World Health Organization, 2009). During the intraerythrocytic stage of the parasite's life cycle, parasite-specific proteins are exported to the erythrocyte cell membrane and surface, resulting in significant modification of these sites. These alterations provide a strategic advantage for the survival of the parasite and are responsible for some of the pathophysiology of malaria (Deitsch & Wellems, 1996; Crabb *et al.*, 1997; Craig & Scherf, 2001). Despite the significance of protein export in *Plasmodium*, its mechanism is still not known (de Koning-Ward *et al.*, 2009).

The mature erythrocyte has no lipid- or protein-trafficking machinery. In erythrocytes infected with *P. falciparum*, the parasite-encoded trafficking machinery is involved in importing nutrients from outside and secreting and exporting proteins and other macromolecules beyond the parasite and the surrounding parasitophorous vacuole membrane to remodel the erythrocyte (Foley & Tilley, 1998; Wiser *et al.*, 1999; van Dooren *et al.*, 2000; Cooke *et al.*, 2000; Boddey *et al.*, 2010). Trelka *et al.* (2000) presented evidence for vesicle-mediated trafficking of *Plasmodium* proteins to the cytosol and surface membrane of infected erythrocytes. Consistent with the above findings, elements of the classical vesicle-mediated secretory pathway for the export of proteins are present within the parasite cytoplasm (Taraschi *et al.*, 2001) and several proteins or genes encoding putative proteins have been identified. These include homologues of endoplasmic reticulum (ER) calcium-binding protein (La Greca *et al.*, 1997), a number of Rab GTPases (reviewed in Quevillon *et al.*, 2003), multiple ADP-ribosylation factors (ARFs; Stafford *et al.*, 1996) and ARF-like proteins (http://plasmodb.org/), ARF GTPase-activating protein (ARFGAP; Senkovich & Chattopadhyay, 2004) and an ARF GTPase-exchange factor (ARFGEF; Baumgartner *et al.*, 2001). Since protein trafficking plays a crucial role in the life cycle of the parasite and the ensuing disease, analyzing the structure and function of the trafficking machinery of *Plasmodium* is of considerable importance. Previously, we have determined the three-dimensional structures of *P. falciparum* Rab6 (Chattopadhyay *et al.*, 2000) and Rab5a (PDB code 3clv; D. Chattopadhyay, A. K. Wernimont, G. Langsley, J. Lew, I. Kozieradzki, D. Cossar, M. Schapira, A. Bochkarev, C. H. Arrowsmith, C. Bountra, J. Weigelt, A. M. Edwards, R. Hui & D. Sukumar, unpublished work).

Table 1
Data-collection and refinement statistics.

Values in parentheses are for the last shell.

Data-collection statistics	
Space group	$C222_1$
Unit-cell parameters (Å)	a = 45.7, b = 147.3, c = 64.2
V_M (Å^3 Da^{-1})	2.58
Solvent content (%)	52
Maximum resolution (Å)	2.50 (2.50–2.59)
Completeness (%)	92.7 (84.5)
R_{merge}	0.092 (0.17)
Overall $\langle I/\sigma(I)\rangle$	12.8
Refinement statistics	
Resolution range (Å)	32.1–2.50 (2.66–2.50)
Reflections	7290
R value	0.189 (0.231)
Free R value	0.253 (0.333)
No. of protein atoms	1475
No. of heteroatoms	34
No. of water molecules	91
Estimated coordinate error	
Luzzati plot (Å)	0.27
Cross-validated Luzzati plot (Å)	0.37
Deviations from ideality	
Bond lengths (Å)	0.006
Bond angles (°)	1.5
Dihedral angles (°)	22.6
Average B factors (Å^2)	
Overall	24.7
Protein	24.4
Heteroatoms	27.1
Water	28.2
Structure	
Ramachandran favored (%)	95.53
Ramachandran outliers (%)	0.00
Rotomer outliers (%)	0.00

One of the main functions of ARF1 is to regulate the trafficking of vesicles that bud from the *cis*-Golgi compartment; this function is dependent on controlled GTP binding and hydrolysis. Binding of GTP activates ARF1, which mediates the recruitment of coat protein I (COPI) proteins to the membrane; COPI proteins dissociate upon hydrolysis of GTP to GDP, a step catalyzed by ARFGAP. ARFGEF subsequently mediates dissociation of GDP. Interestingly, expression of *P. falciparum arf1* mRNA reaches its maximum level at the time of the development of merozoites, so that the peak in *msp1* mRNA expression [for merozoite surface protein 1 (MSP1), the major protein on the merozoite surface] follows that of *arf1* mRNA expression. Based on these data, Stafford *et al.* (1996) speculated that *Pf*ARF1 may be involved in the transport of MSP-1 from the ER on the way to the merozoite surface. Moreover, Leber and coworkers showed an additional role of *Pf*ARF1 in the activation of a potentially unique calcium-signaling mechanism (Leber *et al.*, 2009). ARFs and ARF-like proteins have also been shown to play essential roles in other protozoan parasites (Liendo *et al.*, 2001; Price *et al.*, 2007). Recently, the crystal structure of ARF-like 1 from *Leishmania major* has been deposited in the Protein Data Bank (PDB code 2x77; Fleming *et al.*, 2010). Here, we describe the crystal structure of *P. falciparum* ARF1 (*Pf*ARF1) in the GDP-bound form and compare this structure with those of mammalian ARF1s.

2. Materials and methods

2.1. Expression and purification

The coding sequence for full-length *Pf*ARF1 (residues 1–181; Stafford *et al.*, 1996; gene name ARF1; GenBank accession No. Z80359; *P. falciparum* strain 3D7) fused with an N-terminal GST tag was expressed in *Escherichia coli* BL21 (DE3) cells. The recombinant protein was purified from soluble bacterial extract using affinity chromatography on a GST-Sepharose column (Pharmacia) and was eluted with reduced glutathione in 1× PBS containing 10 m*M* DTT. The purified protein was dialyzed extensively against PBS containing 1 m*M* DTT and was incubated with recombinant factor Xa (Pharmacia) overnight. Cleavage of the GST tag was monitored by SDS–PAGE. Traces of intact fusion protein and the cleaved GST tag were removed by passing the incubation mixture over a small GST-Sepharose column. The unbound protein was concentrated and subjected to size-exclusion chromatography on a Superdex 75 (16/30; Pharmacia) column pre-equilibrated with 50 m*M* Tris–HCl, 0.1 *M* NaCl pH 8.0.

2.2. Crystallization and data collection

Purified *Pf*ARF1 was concentrated by ultrafiltration on an Amicon YM10 membrane to a final concentration of 30 mg ml^{-1}. Initial crystallization conditions were identified using Crystal Screen reagents (Hampton Research) at room temperature and 277 K. Crystals suitable for X-ray diffraction analysis were grown by the hanging-drop vapor-diffusion technique at 277 K using 1.5 *M* ammonium sulfate and 5 m*M* magnesium chloride in 0.1 *M* Tris–HCl buffer pH 7.5. These crystals belong to space group $C222_1$ and have unit-cell parameters a = 45.73, b = 147.28, c = 64.23 Å. There is one molecule per asymmetric unit. X-ray diffraction data were collected using a MAR CCD on synchrotron beamline IMCA 17D at the Advanced Photon Source (APS; Argonne National Laboratory). The calculated values of V_M and the estimated solvent content were 2.58 Å^3 Da^{-1} and 52%, respectively.

2.3. Structure determination and refinement

The structure of *Pf*ARF1 was solved by molecular replacement, using the structure of full-length human ARF1 (hARF1; PDB code 1hur; Amor *et al.*, 1994) as the search model. Although the two switch regions in *Pf*ARF1 are considerably different from those in hARF1, the difference electron-density maps allowed the model to be rebuilt in these regions. Model building was performed using the computer program *Coot* (Emsley & Cowtan, 2004). In the latter stages of refinement, a difference electron-density map clearly showed the positions of the GDP molecule and the magnesium ion (Fig. 1).

The structure was refined by simulated annealing using *CNS* (Brünger *et al.*, 1998) with the stereochemical parameter files defined

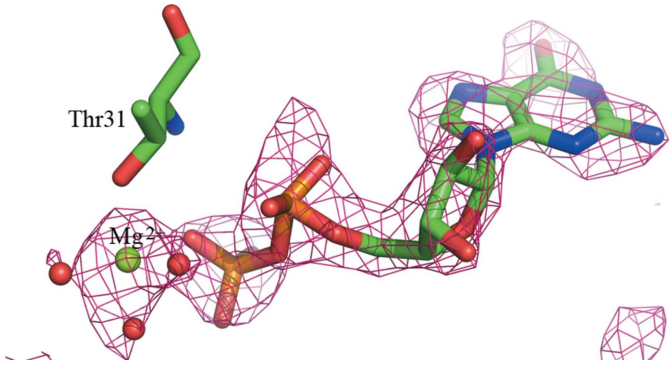

Figure 1
GDP and the environment around the magnesium ion (magenta) with associated electron density. The three water molecules and the Mg^{2+} ion are represented as red spheres and a green sphere, respectively. $F_o - F_c$ electron density calculated before the placement of the GDP molecule (shown in stick representation), Mg^{2+} ion (green sphere) and water molecules (red spheres) is contoured at the 3σ level (shown as a pink mesh). The location of Thr31 is shown as a stick model. Figs. 1, 2, 3(*b*) and 3(*c*) were created with *PyMOL* (DeLano, 2002).

Table 2
Three-dimensional structures of ARF1.

Structure	Species	Comments	Reference	PDB code
ARF1–GDP	Human		Amor *et al.* (1994)	1hur
ARF1–GDP	Rat		Greasley *et al.* (1995)	1rrg, 1rrf
*myr*ARF1–GTP	Yeast		Liu *et al.* (2009)	2ksq (NMR)
*myr*ARF1–GDP	Yeast		Liu *et al.* (2009)	2k5u (NMR)
ARF1Δ17–GDP	Human		Bryson *et al.* (2009)	1u81 (NMR)
ARF1Δ17–GDP	Mouse	Q71L mutant	Shiba *et al.* (2003)	1o3y
ARF-like 1–GDP	*L. major*		Unpublished	2x77
ARF1–GDP	*P. falciparum*		Present work	3lrp
Complexes				
ARF1Δ17–Sec7–BFA	Human ARF1; yeast Sec7		Mossessova *et al.* (1998)	1re0
ARF1Δ17–Sec7	Yeast		Goldberg (1998)	Not deposited
ARF1Δ17–RHOGAP10	Mouse ARF1; human RHOGAP		Monetrey *et al.* (2007)	2j59
ARF1Δ17–Sec7–BFA	Bovine ARF1; human Sec7		Renault *et al.* (2003)	1s9d (supersedes 1r8r)
ARF1Δ17–GDP–mutant Sec7	Bovine ARF1; human Sec7		Renault *et al.* (2003)	1r8s
ARF1Δ17–GDP–ARFGAP	Human ARF1; mouse ARFGAP		Goldberg (1999)	Not deposited
ARF1–GDP–ARFGAP fusion protein	Human	Not a complex (chimeric protein)	Unpublished	3o47

by Engh & Huber (1991). No σ cutoff was applied to the data. 10% of the *Pf*ARF1 data were randomly selected and removed prior to refinement for analysis of the free *R* factor (Brünger, 1992). The progress of the refinement was guided by a decrease in both the conventional and free *R* factors. The 'water_pick' subroutine in the *CNS* program package was used to identify probable water molecules at locations where the peak height in the difference electron-density ($F_o - F_c$) map was at least 3σ and the position satisfied the stereochemical criteria for hydrogen bonding. Individual *B* factors were included in the final refinement. Differences in temperature factors between connected atoms were restrained. Atomic coordinates and structure factors have been deposited in the Protein Data Bank (PDB code 3lrp).

3. Results and discussion

3.1. Structure of *Pf*ARF1

The final *Pf*ARF1 model includes residues 1–181, GDP, magnesium and sulfate ions and 91 water molecules. Validation with *MolProbity* (Chen *et al.*, 2010) revealed a clash score of 19.07 (75th percentile for 271 structures in the resolution range 2.50 ± 0.25 Å) and an overall score of 2.09 (93rd percentile for 6960 structures in the resolution range 2.50 ± 0.25 Å). Table 1 shows a summary of the data-collection and refinement statistics for *Pf*ARF1.

*Pf*ARF1 contains a seven-stranded β-sheet surrounded by six α-helices and its overall structure is similar to those of other ARF1 proteins cocrystallized with GDP (Fig. 2). The electron density for the residues in the GDP-binding site as well as the GDP molecule, the Mg^{2+} ion and associated water molecules was excellent (Fig. 1). The GDP molecule is located in a highly conserved nucleotide-binding pocket. The interaction between GDP and the protein is similar to those in other GTPases. Nine residues are involved in a total of 13 hydrogen-bond contacts and two water molecules contribute three additional hydrogen bonds to the GDP molecule. The square-pyramidal coordination sphere of Mg^{2+} includes the β-phosphate O atom of GDP, the hydroxyl O atom of Thr31 and three water molecules (Fig. 1). One of the coordinating water molecules is hydrogen bonded to Asp67. The equivalent residues in hARF1 (Asp67) and in RasGTPase (Asp57) play a similar role as an 'indirect metal coordinator' (Amor *et al.*, 2004; Halkides *et al.*, 1994). There is a cavity filled with water molecules near the GDP-binding site in the *Pf*ARF1 structure. On reviewing published ARF1 structures, we observe that this cavity and the water molecules are conserved.

A distinctive feature of the structure of the members of the ARF family compared with all other small GTPases is the presence of a helix at the N-terminus. This characteristic amphipathic helix is critical for the biological functions of ARFs. In the native form the N-terminal glycine (residue 2) is modified by the addition of a myristoyl group. This chemical modification is not only essential for membrane association of ARFs, but has also been proposed to play a regulatory role in nucleotide exchange (Liu *et al.*, 2009). In the *Pf*ARF1 structure, as in other non-myristoylated full-length ARF1 structures, the N-terminal loop is well ordered and lies in a hydrophobic cleft parallel to the C-terminal helix.

3.2. Comparison of the *Pf*ARF1 structure with those of other ARF1s

Three-dimensional structures of ARF1s from a number of organisms have been reported in various forms: full-length proteins or truncated versions from which the N-terminal 17 residues have been deleted (Δ17) bound to either GDP or nonhydrolyzable GTP (see

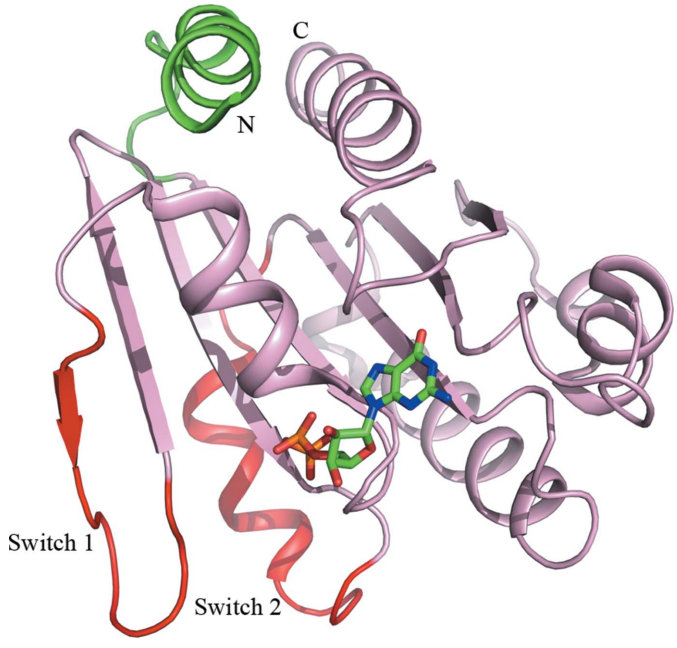

Figure 2
Cartoon drawing of the structure of *Pf*ARF1 (light pink). The switch 1 (residues 42–52) and switch 2 (residues 70–85) regions are colored red; the N-terminal helix (residues 1–17) is shown in green. The GDP molecule is shown as a stick model.

Table 2). While most of these structures contain non-myristoylated protein, solution structures have been determined using myristoylated versions. The amino-acid sequences of ARF1s from various species are homologous (Fig. 3*a*). As expected, the three-dimensional structures of the various ARF1s are highly conserved except in the switch regions, which display significant conformational differences in the GDP-bound and GTP-bound states of ARFs and other small GTPases (Kjeldgaard *et al.*, 1996). The two 'switch regions' are regions of GTPases that have been implicated in their interactions with specific GTP/GDP-exchange proteins (GEPs) and GTPase-activating proteins (GAPs). The overall structure of *Pf*ARF1 is similar to those of full-length ARF1 from human (PDB code 1hur) and rat (PDB codes 1rrf and 1rrg), but shows differences, mainly in the switch 1 (residues 42–52) and switch 2 (70–85) regions, even though these structures are also GDP complexes (Fig. 3*b*). Comparison of the *Pf*ARF1 structure with that of Δ17 human ARF1–GDP, which forms part of a complex with ARFGAP (coordinates obtained from Jonathan Goldberg), revealed no major structural differences outside the switch regions (Goldberg, 1998). Superposition of the *Pf*ARF1 structure with the recently determined structure of *L. major* ARF-like 1 protein (PDB code 2x77) also exhibited a very similar structure except in the switch regions

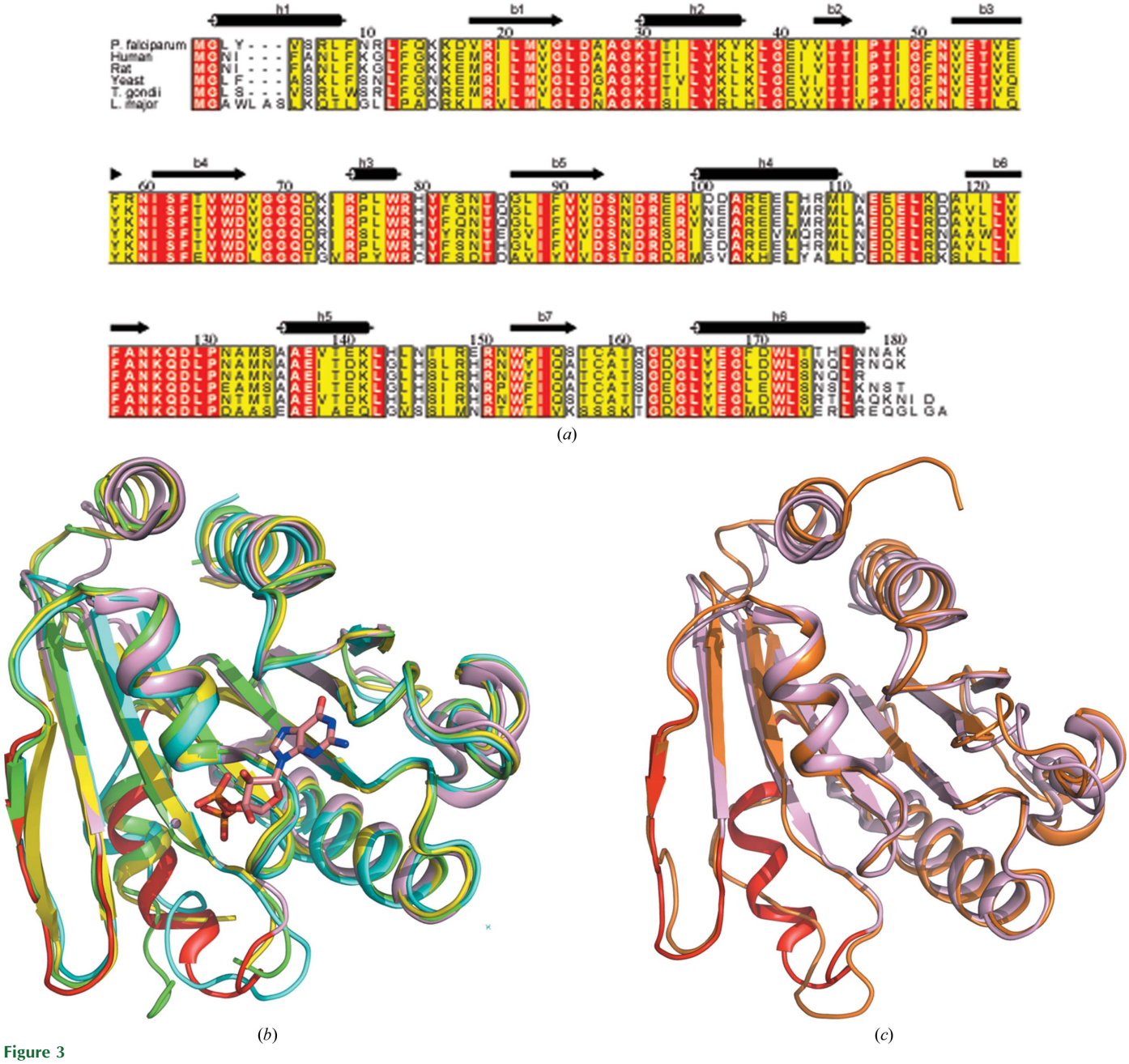

Figure 3
(*a*) Sequence alignment of *Pf*ARF1 with representative ARF1s. The *L. major* sequence is extracted from PDB entry 2x77, which was submitted as ARF-like 1. The human, rat and yeast ARF1 sequences were extracted from PDB entries 1hur, 1rrf and 2k5u, respectively; the *T. gondii* ARF1 sequence was taken from GenBank AAF35891.1. The α-helices and β-strands in *Pf*ARF1 are indicated. This figure was prepared using *ALSCRIPT* (Barton, 1993). (*b*) Superposition of the structure of *Pf*ARF1 (light pink), human full-length ARF1–GDP (1hur; green), rat ARF1–GDP (1rrf; yellow) and human Δ17 ARF1–GDP (cyan). The coordinates for the last structure were taken from the ARF1–ARFGAP complex (Goldberg, 1999) and were obtained from Jonathan Goldberg. (*c*) Superposition of the *Pf*ARF1 structure (light pink) with the *L. major* ARF-like 1 protein structure (orange). The switch 1 and switch 2 regions in the *Pf*ARF1 structure are colored red.

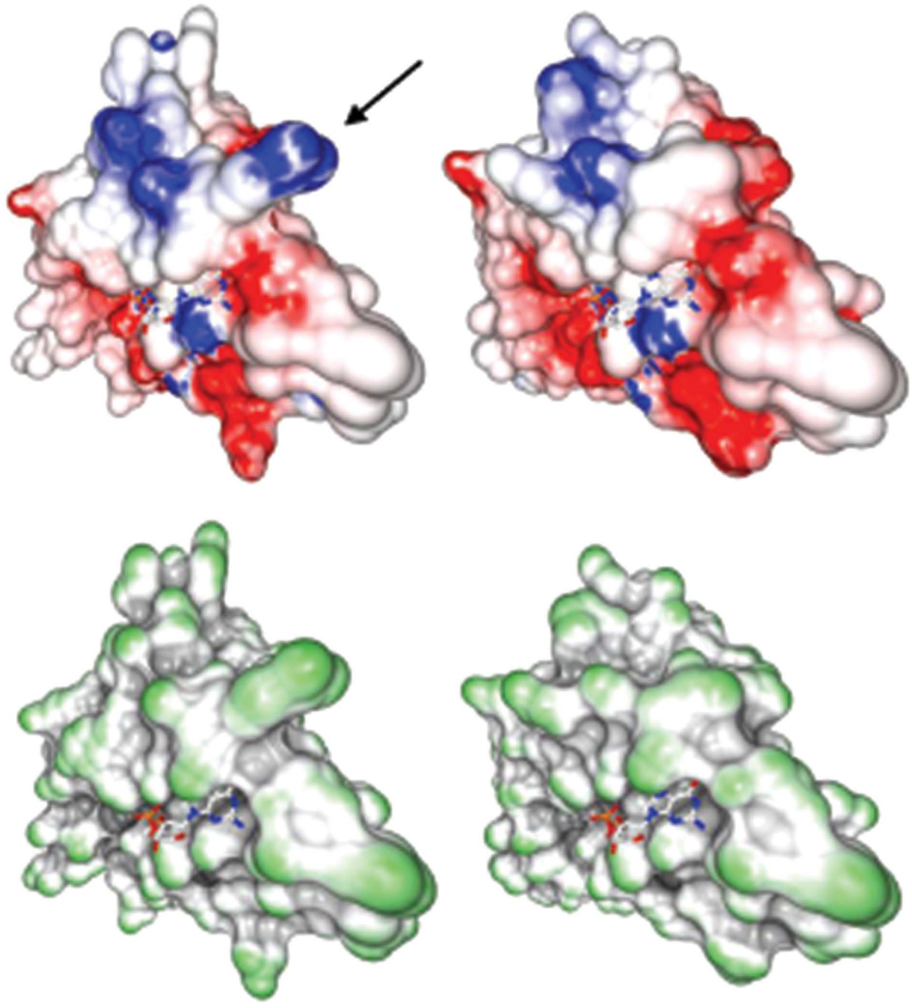

(*a*) (*b*)

Figure 4
Molecular surface of superimposed *Pf*ARF1 (*a*) and full-length hARF1 (*b*) structures drawn using *GRASP*2 (Petrey & Honig, 2003). The top panel shows electrostatic potential: blue indicates regions of positive electrostatic potential, white indicates neutral regions and red indicates regions of negative electrostatic potential. The bottom panel shows surface accessibility (concave regions, gray; convex regions, green; flat areas, white). One of the distinctive regions on the *Pf*ARF1 surface is indicated by an arrow.

(Fig. 3*c*). However, the solution structures of various ARF1s determined using NMR methods differ considerably from the crystal structures (Seidel *et al.*, 2004).

The positions of the GDP molecules in the crystal structures of *Pf*ARF1, hARF1 and rat ARF1 are nearly identical. The fivefold coordination sphere of the Mg^{2+} ion in the present structure is similar to that in the rat ARF1–GDP complex (Greasley *et al.*, 1995). In the structure of human ARF1–GDP (Amor *et al.*, 1994), the Mg^{2+} coordination was reported to be sevenfold in a pentagonal bipyramidal arrangement. Since these crystals were grown in the presence of a high concentration of calcium chloride, the metal ion in this structure may represent Ca^{2+} (Greasley *et al.*, 1995).

The biochemical action of ARFs involves the recognition of and interaction with a number of binding partners. These interactions have been characterized using proteins from various organisms (Goldberg, 1998, 1999; Mossessova *et al.*, 1998; Renault *et al.*, 2003). Although the sites for interaction with partners have not been mapped specifically on *Pf*ARF1, considering the highly conserved primary sequences of ARF1s, particularly in the switch areas, these sites are expected to be similar to those of ARF1s from other organisms. Despite the overall structural similarity and conserved sequences, analyses of the molecular surfaces of hARF1 and *Pf*ARF1 show areas that are significantly different in terms of their surface accessibility and distribution of electrostatic potential (Fig. 4). One such region (shown in Fig. 4) contains Arg162. In human, rat and yeast ARF1 a serine residue occupies the equivalent position. Alignment of amino-acid sequences of ARF1 proteins from multiple protozoan parasites shows either a serine or a threonine residue at this position, but an arginine is present as a signature residue in all species of *Plasmodium*. Further molecular and structural data will be necessary in order to determine whether these sites on the *Pf*ARF1 surface represent areas for specific intermolecular interactions. Interestingly, the predicted primary sequence of *Plasmodium* ARFGEF suggests a novel structural organization for this molecule (Baumgartner *et al.*, 2001). Future studies may reveal new protein–protein interaction sites at the *Pf*ARF1–ARFGEF interface that could be of interest for therapeutic development.

We thank Dr Esther Suswam for assistance with *Pf*ARF1 purification. The coordinates of the human Δ17 ARF1–GDP–ARFGAP complex were kindly provided by Dr Jonathan Goldberg. We thank

the staff of the IMCA beamline. Use of the Argonne National Laboratory IMCA beamline at the Advanced Photon Source was supported by the US Department of Energy, Office of Energy Research under contract No. W-31-109-ENG-38.

References

Amor, C., Harrison, D., Kahn, R. & Ringe, D. (1994). *Nature (London)*, **372**, 704–708.

Barton, G. J. (1993). *Protein Eng.* **6**, 37–40.

Baumgartner, F., Wiek, S., Paprotka, K., Zauner, S. & Lingelbach, K. (2001). *Mol. Microbiol.* **41**, 1151–1158.

Boddey, J. A., Hodder, A. N., Günther, S., Gilson, P. R., Patsiouras, H., Kapp, E. A., Pearce, J. A., de Koning-Ward, T. F., Simpson, R. J., Crabb, B. S. & Cowman, A. F. (2010). *Nature (London)*, **463**, 627–631.

Brünger, A. T. (1992). *Nature (London)*, **355**, 472–475.

Brünger, A. T., Adams, P. D., Clore, G. M., DeLano, W. L., Gros, P., Grosse-Kunstleve, R. W., Jiang, J.-S., Kuszewski, J., Nilges, M., Pannu, N. S., Read, R. J., Rice, L. M., Simonson, T. & Warren, G. L. (1998). *Acta Cryst.* D**54**, 905–921.

Chattopadhyay, D., Langsley, G., Carson, M., Recacha, R., DeLucas, L. & Smith, C. (2000). *Acta Cryst.* D**56**, 937–944.

Cooke, B., Coppel, R. & Wahlgren, M. (2000). *Parasitol. Today*, **16**, 416–420.

Crabb, B. S., Cooke, B. M., Reeder, J. C., Waller, R. F., Caruana, S. R., Davern, K. M., Wickham, M. E., Brown, G. V., Coppel, R. L. & Cowman, A. F. (1997). *Cell*, **89**, 287–296.

Craig, A. & Scherf, A. (2001). *Mol. Biochem. Parasitol.* **115**, 129–143.

Chen, V. B., Arendall, W. B., Headd, J. J., Keedy, D. A., Immormino, R. M., Kapral, G. J., Murray, L. W., Richardson, J. S. & Richardson, D. C. (2010). *Acta Cryst.* D**66**, 12–21.

Deitsch, K. W. & Wellems, T. E. (1996). *Mol. Biochem. Parasitol.* **76**, 1–10.

DeLano, W. L. (2002). *PyMOL.* http://www.pymol.org.

Dooren, G. G. van, Waller, R. F., Joiner, K. A., Roos, D. S. & McFadden, G. I. (2000). *Parasitol. Today*, **16**, 421–427.

Emsley, P. & Cowtan, K. (2004). *Acta Cryst.* D**60**, 2126–2132.

Engh, R. A. & Huber, R. (1991). *Acta Cryst.* A**47**, 392–400.

Fleming, J. R., Dawson, A. & Hunter, W. N. (2010). *Mol. Biochem. Parasitol.* **174**, 141–144.

Foley, M. & Tilley, L. (1998). *Int. J. Parasitol.* **28**, 1671–1680.

Goldberg, J. (1998). *Cell*, **95**, 237–248.

Goldberg, J. (1999). *Cell*, **96**, 893–902.

Greasley, S., Jhoti, H., Teahan, C., Solari, R., Fensome, A., Thomas, G. M. H., Cockcroft, S. & Bax, B. (1995). *Nature Struct. Biol.* **2**, 797–806.

Halkides, C. J., Farrar, C. T., Larsen, R. G., Redifield, A. G. & Singel, D. J. (1994). *Biochemistry*, **33**, 4019–4035.

Kjeldgaard, M., Nyborg, J. & Clark, B. F. C. (1996). *FASEB J.* **10**, 1347–1368.

La Greca, N., Hibbs, A. R., Riffkin, C., Foley, M. & Tilley, L. (1997). *Mol. Biochem. Parasitol.* **89**, 283–293.

Leber, W., Skippen, A., Fivelman, Q. L., Bowyer, P. W., Cockcroft, S. & Baker, D. A. (2009). *Int. J. Parasitol.* **39**, 645–653.

Liendo, A., Stedman, T. T., Ngô, H. M., Chaturvedi, S., Hoppe, H. C. & Joiner, K. A. (2001). *J. Biol. Chem.* **276**, 18272–18281.

Liu, Y., Kahn, R. A. & Prestegard, J. H. (2009). *Structure*, **17**, 79–87.

Menetrey, J., Perderiset, M., Cicolari, J., Dubois, T., El Khatib, N., El Khadali, F., Franco, M., Chavrier, P. & Houdusse, A. (2007). *EMBO J.* **26**, 1953–1962.

Mossessova, E., Gulbis, J. M. & Goldberg, J. (1998). *Cell*, **92**, 415–423.

Petrey, D. & Honig, B. (2003). *Methods Enzymol.* **374**, 492–509.

Price, H. P., Stark, M. & Smith, D. F. (2007). *Mol. Biol. Cell*, **18**, 864–873.

Quevillon, E., Spielmann, T., Brahimi, K., Chattopadhyay, D., Yeraman, E. & Langsley, G. (2003). *Gene*, **306**, 13–25.

Renault, L., Guibert, B. & Cherfils, J. (2003). *Nature (London)*, **426**, 525–530.

Seidel, R. D., Amor, J. C., Kahn, R. A. & Prestegard, J. H. (2004). *J. Biol. Chem.* **46**, 48307–48318.

Senkovich, O. & Chattopadhyay, D. (2004). *Biochim. Biophys. Acta*, **1698**, 127–130.

Shiba, T., Kawasaki, M., Takatsu, H., Nogi, T., Matsugaki, N., Igarashi, N., Suzuki, M., Kato, R., Nakayama, K. & Wakatsuki, S. (2003). *Nature Struct. Biol.* **10**, 386–393.

Stafford, W. H., Stockley, R. W., Ludbrook, S. B. & Holder, A. A. (1996). *Eur. J. Biochem.* **242**, 104–113.

Taraschi, T. F., Trelka, D., Martinez, S., Schneider, T. & O'Donnell, M. E. (2001). *Int. J. Parasitol.* **31**, 1381–1391.

Trelka, D. P., Schneider, T. G., Reeder, J. C. & Taraschi, T. F. (2000). *Mol. Biochem. Parasitol.* **106**, 131–145.

Wiser, M. F., Lanners, H. N. & Bafford, R. A. (1999). *Parasitol. Today*, **15**, 194–198.

World Health Organization (2009). *World Malaria Report.* Geneva: World Health Organization. http://www.who.int/malaria/world_malaria_report_2009/en/.